Observation of Phase Defects in Quasi-2D Bose-Einstein Condensates

Sabine Stock, Zoran Hadzibabic, Baptiste Battelier, Marc Cheneau, Jean Dalibard

Observation of Phase Defects in Quasi-2D Bose-Einstein Condensates

Sabine Stock, Zoran Hadzibabic, Baptiste Battelier, Marc Cheneau, and Jean Dalibard
Laboratoire Kastler Brossel, 24 rue Lhomond, 75005 Paris, France*
(Dated: 13th November 2005)

We have observed phase defects in quasi-2D Bose-Einstein condensates close to the condensation temperature. Either a single or several equally spaced condensates are produced by selectively evaporating the sites of a 1D optical lattice. When several clouds are released from the lattice and allowed to overlap, dislocation lines in the interference patterns reveal nontrivial phase defects.

PACS numbers: 03.75.Lm, 32.80.Pj, 67.40.Vs

Low dimensional bosonic systems have very different coherence properties than their three dimensional (3D) counterparts. In a spatially uniform one dimensional (1D) system, a Bose-Einstein condensate (BEC) cannot exist even at zero temperature. In two dimensions (2D) a BEC exists at zero temperature, but phase fluctuations destroy the long range order at any finite temperature. At low temperatures the system is superfluid and the phase fluctuations can be described as bound vortex-antivortex pairs. At the Kosterlitz-Thouless (KT) transition temperature [1, 2, 3] the unbinding of the pairs becomes favorable and the system enters the normal state.

In recent years, great efforts have been made to study the effects of reduced dimensionality in trapped atomic gases [4]. In both 1D and 2D, the density of states in a harmonic trap allows for Bose-Einstein condensation at finite temperature. In contrast to 1D and elongated 3D systems [5, 6, 7, 8, 9, 10, 11, 12, 13], the coherence properties of 2D atomic BECs have so far been explored only theoretically [14, 15, 16, 17]. In previous experiments, quasi-2D BECs [6, 18, 19, 20] or ultracold clouds [21] were produced in specially designed "pancake" trapping potentials. The sites of a 1D optical lattice usually also fulfill the criteria for 2D trapping [22, 23, 24, 25]; the difficulty in these systems is to suppress tunneling between the sites, and to address or study them independently [26, 27].

In this Letter, we report the production of an array of individually addressable quasi-2D BECs. By selectively evaporating the atoms from the sites of a 1D optical lattice, we can produce either a single or several equally spaced condensates. The distinct advantage of this approach is that it opens the possibility to study the phase structures in quasi-2D BECs interferometrically. We have observed interference patterns which clearly reveal the presence of phase defects in condensates close to the ideal gas Bose-Einstein condensation temperature. We discuss the possible underlying phase configurations.

Our experiments start with an almost pure ^{87}Rb condensate with 4×10^5 atoms in the $F = m_F = 2$ hyperfine state, produced by radio-frequency (rf) evaporation in a cylindrically symmetric Ioffe-Pritchard (IP) magnetic trap. The trapping frequencies are $\omega_z/2\pi = 12\,\mathrm{Hz}$ axially, and $\omega_\perp/2\pi = 106\,\mathrm{Hz}$ radially, leading to cigar-shaped condensates with a Thomas-Fermi length of $90\,\mu$m and a diameter of $10\,\mu$m.

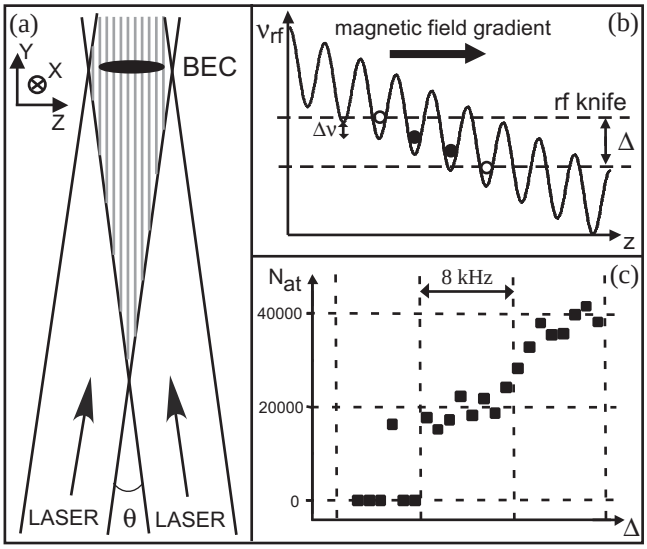

Figure 1: An array of individually addressable quasi-2D BECs. (a) A 1D optical lattice splits a cigar-shaped 3D condensate into 15 - 30 independent quasi-2D BECs. (b) A magnetic field gradient along the lattice axis allows us to selectively address the sites by an rf field. We evaporate the atoms from all the sites except those within a frequency gap Δ. (c) Steps in the BEC atom number N_{at} as a function of Δ, corresponding to 0, 1 and 2 sites spared from evaporation. Each data point represents a single measurement.

After creation of the BEC we ramp up the periodic potential of a 1D optical lattice, which splits the 3D condensate into an array of independent quasi-2D BECs (see Fig. 1(a) and [24]). The lattice is superimposed on the magnetic trapping potential along the long axis (z) of the cigar. Two horizontal laser beams of wavelength $\lambda = 532\,\mathrm{nm}$ intersect at a small angle θ to create a standing wave with a period of $d = \lambda/[2\sin(\theta/2)]$. The blue-detuned laser light creates a repulsive potential for the atoms, which accumulate at the nodes of the standing wave, with the radial confinement being provided by the magnetic potential. Along z, the lattice potential has the shape $V(z) = V_0 \cos^2(\pi z/d)$, with $V_0/h \approx 50\,\mathrm{kHz}$.

For the work presented here we have used two lattice periods, $d_1 = 2.7\,\mu$m and $d_2 = 5.1\,\mu$m. The respec-

tive oscillation frequencies along z are $\omega_1/2\pi = 4.0\,\mathrm{kHz}$ and $\omega_2/2\pi = 2.1\,\mathrm{kHz}$. At the end of the experimental cycle (described below), the BEC atom numbers in the most populated, central sites are $N_1 \approx 10^4$ and $N_2 \approx 2\times10^4$. We numerically solve the Gross-Pitaevskii equation to get the corresponding chemical potentials $\mu_1/h = 2.2\,\mathrm{kHz}$ and $\mu_2/h = 2.5\,\mathrm{kHz}$, where the $\hbar\omega_{1,2}/2$ zero-point offset is suppressed in our definition of μ. In the smooth crossover from 3D to 2D, the condensates in the shorter period lattice are thus well in the 2D regime with $\mu_1/(\hbar\omega_1) = 0.6$, while for the clouds in the longer period lattice this ratio is 1.2.

Since the radial trapping is purely magnetic, we can remove atoms from the lattice by rf induced spin-flips to untrapped Zeeman states. In order to address the lattice sites selectively, we apply a magnetic field gradient b' along z [27, 28]. This creates an energy gradient along the lattice direction, and splits the resonant frequencies for evaporation of atoms from two neighboring sites by $\Delta\nu_{1,2} = \mu_\mathrm{B} b' d_{1,2}/(2h)$, where μ_B is the Bohr magneton (Fig. 1(b)). We use gradients up to 26 G/cm, corresponding to $\Delta\nu_1 = 5\,\mathrm{kHz}$ and $\Delta\nu_2 = 9\,\mathrm{kHz}$. These splittings are larger than the chemical potentials $\mu_{1,2}$, and the rf Rabi frequency ($\approx 2\,\mathrm{kHz}$). The lattice sites can thus be addressed individually.

The experimental routine to produce an adjustable number of condensates starts with a slow, 200 ms ramp-up of the gradient b'. As illustrated in Fig. 1(b), we then evaporate the atoms from both ends of the cigar, sparing only the central sites within a variable rf frequency gap Δ. We perform this evaporation in 100 ms, switch off the rf field, and ramp b' back to zero in another 200 ms [29]. During this time, some heating of the remaining clouds occurs, and they reach a temperature slightly below the condensation temperature, as we discuss in detail below.

To verify that we can address the lattice sites individually, we measure the total number of condensed atoms left in the trap as a function of Δ. An example of such a plot is shown in Fig. 1(c) for $d_2 = 5.1\,\mu\mathrm{m}$ and $b' = 22\,\mathrm{G/cm}$. The magnetic and optical trap were switched off simultaneously and the atomic density distribution was recorded by absorption imaging along z after 18 ms of time-of-flight (TOF) expansion. The atom number increases in steps of $N_2 = 2\times10^4$ every 8 kHz, in agreement with the expected $\Delta\nu_2$. We see three clear plateaus corresponding to 0, 1 and 2 sites spared from evaporation. For the shorter lattice period the frequency splitting is comparable to the chemical potential. This results in some rounding off of the steps, but the plateaus remain visible.

In the first set of experiments, we have characterized the free expansion of a single quasi-2D BEC [30]. The clouds were released from the $5.1\,\mu\mathrm{m}$ period lattice and imaged after up to 18 ms of TOF. We extract the axial (l) and the radial (w) rms size of the cloud from gaussian fits to the density distribution. As might be expected, the observed expansion is predominantly one-dimensional, along the axial direction. For short expansion times, $t \leq 3\,\mathrm{ms}$, the apparent axial size is limited by our imaging resolution, but for longer times it follows the linear scaling $l = vt$, with $v = 2.7\,\mathrm{mm/s}$. This value is comparable to the calculated velocity in the harmonic oscillator ground state along z, $v_g = \sqrt{\hbar\omega_2/(2m)} = 2.1\,\mathrm{mm/s}$, where m is the atomic mass. We find that the radial expansion can be described by the empirical law $w = w_0\sqrt{1+(t/t_0)^2}$, with $w_0 = 4.4\,\mu\mathrm{m}$ and $t_0 = 5.7\,\mathrm{ms}$. The same law describes the radial expansion of a cigar-shaped 3D condensate, with $t_0 = \omega_\perp^{-1}$ [31], where $\omega_\perp^{-1} = 1.5\,\mathrm{ms}$ for our trap. The radial expansion of our 2D gas is slower by a factor of ≈ 4 compared to the 3D case, because the fast axial expansion results in an almost sudden ($\omega_2^{-1} = 76\,\mu\mathrm{s}$) decrease of the atomic density, and only a small fraction of the interaction energy is converted into radial velocity.

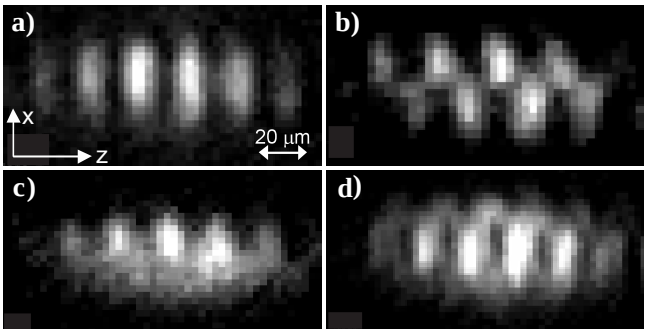

Figure 2: Phase defects in quasi-2D condensates. Interference of four (a-c) and seven (d) independent BECs is observed 12 ms after release from the $2.7\,\mu\mathrm{m}$ period lattice. Dislocation lines in the interference patterns (b-d) reveal the presence of phase defects in quasi-2D condensates.

In the second set of experiments, we have studied interference of independent quasi-2D BECs. Between two and eight clouds were released from the $2.7\,\mu\mathrm{m}$ period lattice and allowed to expand and overlap [32]. The resulting interference patterns were recorded by absorption imaging along the radial direction y. Due to the finite imaging resolution we observe only the first harmonic of the interference pattern with period $ht/(md_1)$. Each image is thus the incoherent sum of the pairwise interferences of nearest-neighbor condensates.

Interference of equally spaced, independent BECs produces straight interference fringes (Fig. 2(a)) as long as each BEC has a spatially uniform phase [24, 33]. The main result of this paper is the observation of topologically different patterns, which reveal the presence of phase defects in quasi-2D condensates. Striking examples are "zipper" patterns (Fig. 2(b)), where the fringe phase changes abruptly by π across a dislocation line parallel to z. On both sides of the dislocation, the fringe contrast is as high as in Fig. 2(a). We also observe "comb" patterns (Fig. 2(c)), which show a dislocation with high fringe contrast on one side of the line, and vanishing on the other. Finally, we sometimes see "braid" structures with two dislocation lines (Fig. 2(d)). Single dislocations

(zippers and combs) are clearly visible in about 15% of 200 experiments with four interfering clouds [34]. To verify that the occurrence of defects is an equilibrium property of the system, we have checked that dislocations are still observed when holding the clouds in the lattice for 500 ms after ramping down the gradient b'.

The simplest phase configuration which can produce a sharp dislocation line is a single vortex in one of the condensates (see also [35, 36, 37, 38, 39]). In the case of two interfering BECs, one can show that a centered vortex always leads to a zipper pattern (see a simulation of the expected pattern in Fig. 3 (a)). The zipper is indeed the only type of dislocation we clearly observe with two clouds. When more than two BECs interfere, the presence of a single vortex can result both in a zipper and in a comb pattern, depending on the phases of the other condensates. In Fig. 3 (b) we show a numerical simulation with four BECs leading to a comb. Increasing the number of interfering BECs enhances the probability that some of them contain defects [40], but the interpretation of images also becomes increasingly difficult. Further, for a large number of clouds, a single defect will not produce a clear dislocation line in the first harmonic of the interference pattern, because it affects only the interference with the two neighboring BECs. Already with four clouds, only half of 100 simulations with a vortex show clear zipper- or comb-type dislocations. The other half shows weaker dislocations which are not easily distinguishable from straight interference fringes.

Despite the agreement between simulations involving a vortex and the observed patterns, we point out that it is in general not possible to unambiguously deduce the underlying phase configuration from an interference image. For example, a dislocation line could also come from a dark soliton, where the phase of one of the BECs changes by π across a line parallel to the imaging axis. In future experiments simultaneous imaging along a second radial direction could allow us to discriminate between different possible phase structures leading to the observed interference patterns.

So far we could not observe a clear signature of vortices in images of single condensates taken along the axial direction z. We suspect that this is difficult because of the expansion properties of a 2D gas. Rotating 3D BECs, in which vortices are readily detected after TOF [41], expand mostly radially, while our clouds expand mostly axially. Therefore, any small misalignment with the imaging axis will significantly reduce the contrast. Interferometric detection along a radial direction offers a fundamentally superior signal, because a localized defect affects the appearance of the whole image.

It is important to assess the temperature of the clouds in which the observed phase defects appear. Precise thermometry at the end of the experimental cycle is difficult, because the thermal cloud is very dilute. However, we can estimate lower and upper bounds for the temperature. During the 500 ms selective evaporation routine, the clouds are heated due to three-body recombination, and the only constant source of cooling is the finite lattice depth; atoms with an energy larger than V_0 are accelerated away by the magnetic field gradient (Fig. 1(b)). Assuming the largest realistic evaporation parameter $\eta = V_0/(kT) = 10$, we get a lower bound for the temperature $T_{\min} \approx 250\,\mathrm{nK}$. To get an upper bound we note that at the beginning of the experiment the condensed fraction is certainly above 50%. During the experimental cycle the number of condensed atoms in the remaining sites drops by a factor of ≈ 2. This means that, even if we neglect losses in the total atom number, the final condensed fraction cannot be less than 25%. Using the measured number of condensed atoms and integrating the Bose distribution over the density of states in the lattice, we get $T_{\max} \approx 500\,\mathrm{nK}$. Since the number of thermal atoms is different at $T_{\min}$ and $T_{\max}$, the two bounds correspond to different condensation temperatures T_c, and the estimated temperature range is more clearly expressed as $0.7 \leq T/T_c \leq 0.9$. In this temperature range $kT \gtrsim \hbar\omega_{1,2}$, so the thermal clouds are not fully in the 2D regime.

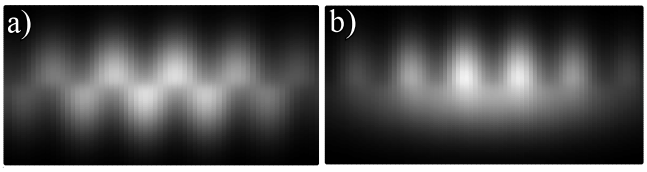

Figure 3: Examples of numerical simulations of two (a) and four (b) interfering condensates. In both cases one randomly chosen BEC has a phase factor $e^{i\varphi}$ corresponding to a centered vortex, and the others have randomly chosen uniform phases. For simplicity, we model the clouds as gaussian wave packets and neglect interactions during the expansion. The images are convolved with a gaussian of 4 μm rms width to simulate the finite imaging resolution.

The fact that the clouds are close to T_c is probably essential for the understanding of our observations, and a systematic temperature study will be the subject of future work. The probability for a thermal excitation of the system into a vortex state is $\propto e^{-F/kT}$, where $F = E - TS$ is the free energy associated with the excitation, E the energy, and S the entropy. Here we estimate the conditions for F/kT to be of order unity. For a vortex in the center of the condensate, $E \sim N\left[(\hbar\omega_\perp)^2/\mu\right]\ln(R/\xi)$ [37], where N is the BEC atom number, R the size of the condensate, and $\xi = \hbar/\sqrt{2m\mu}$ the size of the vortex core. Equivalently, $E/(kT) \sim (1/2)\, n_0\lambda^2 \ln(R/\xi)$, where n_0 is the peak 2D atom density and λ is the thermal wavelength $h/\sqrt{2\pi mkT}$. The number of distinguishable positions for a straight vortex of size ξ in a region of size R is $\sim R^2/\xi^2$, and the associated entropy is $S/k \sim 2\ln(R/\xi)$. In this estimate $F/kT \propto \left(n_0\lambda^2 - 4\right)$ vanishes for $n_0\lambda^2 = 4$. In our experiment $n_0\lambda^2 \sim 10 - 20$ is a few times higher than this

value. However already this crude agreement suggests that the thermal excitation of vortices might be possible in our system.

Thermal excitation of a tightly bound vortex-antivortex pair [17] is more likely than that of a single vortex. In that case the entropy is comparable and the energy is typically lower by the logarithmic factor $\ln(R/\xi)$, in our case ~ 4. These pairs are difficult to detect with our interferometric scheme since they create only small phase slips in the fringe pattern. However they can play a significant role by screening the velocity field of a single vortex, thus lowering its energy and making its appearance more likely [1].

The fact that $\ln(R/\xi)$ is not large compared to 1 underlines the mesoscopic nature of our system. In a homogeneous 2D system with $R \to \infty$, both the energy and the entropy of a free vortex diverge as $\ln(R)$, and the two contributions to the free energy cancel at the KT transition temperature $T_{\rm KT}$. Below $T_{\rm KT}$ only vortex-antivortex pairs are present, while above $T_{\rm KT}$ a large density of free vortices appears and suppresses superfluidity. In our case, we expect this phase transition to be replaced by a gradual increase of the average number of free vortices with temperature. For $F \sim kT$, the vortex number can show large fluctuations and two condensates produced under identical experimental conditions can have qualitatively different wave functions.

In conclusion, by selectively addressing individual sites of a 1D lattice, we have produced both a single and several equally spaced quasi-2D BECs. We have characterized the free expansion of a single BEC, and have interferometrically observed clear evidence for the presence of phase defects in about 10% of eight hundred condensates. While our observations can be explained by the presence of thermally excited vortices in the system, this does not exclude other scenarios and we hope that our experiments will stimulate further theoretical work.

We thank the ENS "cold atoms" group for useful discussions. S.S. acknowledges support from the Studienstiftung des deutschen Volkes and the DAAD, and Z.H. from a Chateaubriand grant and the EU (Contract No. MIF1-CT-2005-00793). This work is partially supported by CNRS, Région Ile de France, and ACI Nanoscience.

[1] J. M. Kosterlitz and D. J. Thouless, J. Phys. C: Solid State Physics **6**, 1181 (1973).
[2] D. J. Bishop and J. D. Reppy, Phys. Rev. Lett. **40**, 1727 (1978).
[3] A. I. Safonov, S. A. Vasilyev, I. S. Yasnikov, I. I. Lukashevich, and S. Jaakkola, Phys. Rev. Lett. **81**, 4545 (1998).
[4] *Quantum gases in low dimensions*, edited by L. Pricoupenko, H. Perrin and M. Olshanii (EDP Science, 2004).
[5] F. Schreck *et al.*, Phys. Rev. Lett. **87**, 080403 (2001).
[6] A. Görlitz *et al.*, Phys. Rev. Lett. **87**, 130402 (2001).
[7] S. Dettmer *et al.*, Phys. Rev. Lett. **87**, 160406 (2001).
[8] I. Shvarchuck *et al.*, Phys. Rev. Lett. **89**, 270404 (2002).
[9] S. Richard *et al.*, Phys. Rev. Lett. **91**, 010405 (2003).
[10] B. Laburthe Tolra *et al.*, Phys. Rev. Lett. **92**, 190401 (2004).
[11] T. Stöferle, H. Moritz, C. Schori, M. Köhl, and T. Esslinger, Phys. Rev. Lett. **92**, 130403 (2004).
[12] B. Paredes *et al.*, Nature **429**, 277 (2004).
[13] T. Kinoshita, T. Wenger, and D. S. Weiss, Science **305**, 1125 (2004).
[14] D. S. Petrov, M. Holzmann, and G. V. Shlyapnikov, Phys. Rev. Lett. **84**, 2551 (2000).
[15] Y. Kagan, V. A. Kashurnikov, A. V. Krasavin, N. V. Prokof'ev, and B. V. Svistunov, Phys. Rev. A **61**, 043608 (2000).
[16] J. O. Andersen, U. A. Khawaja, and H. T. C. Stoof, Phys. Rev. Lett. **88**, 070407 (2002).
[17] T. P. Simula, M. D. Lee, and D. A. W. Hutchinson, cond-mat/0412512 (2004).
[18] V. Schweikhard, I. Coddington, P. Engels, V. P. Mogendorff, and E. A. Cornell, Phys. Rev. Lett. **92**, 040404 (2004).
[19] D. Rychtarik, B. Engeser, H.-C. Nägerl, and R. Grimm, Phys. Rev. Lett. **92**, 173003 (2004).
[20] N. L. Smith, W. H. Heathcote, G. Hechenblaikner, E. Nugent, and C. J. Foot, Journal of Physics B **38**, 223 (2005).
[21] Y. Colombe, E. Knyazchyan, O. Morizot, B. Mercier, V. Lorent, and H. Perrin, Europhys. Lett. **67**, 593 (2004).
[22] C. Orzel, A. K. Tuchman, M. L. Fenselau, M. Yasuda, and M. A. Kasevich, Science **291**, 2386 (2001).
[23] S. Burger *et al.*, Europhys. Lett. **57**, 1 (2002).
[24] Z. Hadzibabic, S. Stock, B. Battelier, V. Bretin, and J. Dalibard, Phys. Rev. Lett. **93**, 180403 (2004).
[25] M. Köhl, H. Moritz, T. Stöferle, C. Schori, and T. Esslinger, J. Low. Temp. Phys. **138**, 635 (2005).
[26] H. Ott *et al.*, Phys. Rev. Lett **93**, 120407 (2004).
[27] D. Schrader *et al.*, Phys. Rev. Lett. **93**, 150501 (2004).
[28] The gradient is produced by a pair of coils in anti-Helmholtz configuration. Their quadrupole field splits the radial trap frequencies $\omega_{x,y}$ by 20% for $b' = 26\,\mathrm{G/cm}$.
[29] To improve addressability we reduce the gravitational sag to $6\,\mu$m for the evaporation of individual sites. This is achieved by ramping the axial bias field of the IP trap simultaneously with the gradient ramps.
[30] G. Hechenblaikner, J. M. Krueger, and C. J. Foot, Phys. Rev. A **71**, 013604 (2005).
[31] Y. Castin and R. Dum, Phys. Rev. Lett. **77**, 5315 (1996).
[32] Comparable results were obtained in experiments performed with the lattice of period $d_2 = 5.1\,\mu$m.
[33] M. R. Andrews *et al.*, C. G. Townsend, Science **275**, 637 (1997).
[34] Another 15 % of images show significantly reduced contrast or patterns which are hard to classify.
[35] E. L. Bolda and D. F. Walls, Phys. Rev. Lett. **81**, 5477 (1998).
[36] J. Tempere and J. T. Devreese, Solid State Commun. **108**, 993 (1998).
[37] Y. Castin and R. Dum, Eur. Phys. J. D **7**, 399 (1999).
[38] S. Inouye *et al.*, Phys. Rev. Lett. **87**, 080402 (2001).
[39] F. Chevy, K. Madison, V. Bretin, and J. Dalibard, Phys. Rev. A **64**, 031601(R) (2001).
[40] For example, the braid patterns with two dislocation lines were observed only with more than four clouds.
[41] K. W. Madison, F. Chevy, W. Wohlleben, and J. Dal-

ibard, Phys. Rev. Lett. **84**, 806 (2000).